Electronic Supplementary Material (ESI) for Nanoscale Horizons.


# Core-shell GaN/AlGaN nanowires grown by selective area epitaxy

**Sonachand Adhikari[1,2 *], Felipe Kremer[3], Mykhaylo Lysevych[4], Chennupati Jagadish[1,5], Hark Hoe Tan[1,5 *]**

[1]Department of Electronic Materials Engineering, Research School of Physics, The Australian National University, Canberra, Australian Capital Territory 2600, Australia

[2]Council of Scientific & Industrial Research - Central Electronics Engineering Research Institute, Pilani, Rajasthan 333031, India

[3]Centre for Advanced Microscopy, The Australian National University, Canberra, Australian Capital Territory 2600, Australia

[4]Australian National Fabrication Facility ACT Node, Research School of Physics, The Australian National University, Canberra, Australian Capital Territory 2600, Australia

[5]Australian Research Council Centre of Excellence for Transformative Meta-Optical Systems, Research School of Physics, The Australian National University, Canberra, Australian Capital Territory 2600, Australia

sonachand.adhikari@anu.edu.au; hoe.tan@anu.edu.au

## 1. Bandgap calculation for strained AlGaN on GaN using elastic constants and deformation potential

Bandgap energies of strained AlGaN have been calculated using the lattice parameters, bandgap energies, elastic constants, and deformation potentials listed in Table S1.

Table S1. Lattice parameters, bandgap energies, elastic constants, and deformations potentials of binary III-nitrides.

| | AlN | GaN | InN |
|---|---|---|---|
| Lattice parameter and $E_g$ | | | |
| $a$ (Å) | 3.112 | 3.190 | 3.540 |
| $c$ (Å) | 4.982 | 5.189 | 5.706 |
| $E_g$ (eV) | 6.2 | 3.42 | 0.7 |
| Elastic constants (GPa) | | | |
| $C_{11}$ | 396 | 367 | 223 |
| $C_{12}$ | 137 | 135 | 115 |
| $C_{13}$ | 108 | 103 | 92 |

| | | | |
|---|---|---|---|
| $C_{33}$ | 373 | 405 | 224 |
| $C_{44}$ | 116 | 95 | 48 |
| $B$ | 207 | 202 | 141 |
| Deformation potentials (eV) | | | |
| $a_{cz}$ - $D_1$ | -4.36 | -6.07 | -3.64 |
| $a_{ct}$ - $D_2$ | -12.35 | -8.88 | -4.58 |
| $D_3$ | 9.17 | 5.38 | 2.68 |
| $D_4$ | -3.72 | -2.69 | -1.78 |
| $D_5$ | -2.93 | -2.56 | -2.07 |
| $D_6$ | -4.58 | -3.88 | -3.02 |

The lattice parameters, $a$ and $c$, elastic constants, $C$, and deformation potentials, $D$, for the ternary AlGaN alloys were calculated using the values of AlN and GaN by linear interpolation as

$$a_{AlGaN} = a_{AlN} \times x + a_{GaN} \times (1 - x)$$

$$c_{AlGaN} = c_{AlN} \times x + c_{GaN} \times (1 - x)$$

$$C_{AlGaN} = C_{AlN} \times x + C_{GaN} \times (1 - x)$$

$$D_{AlGaN} = D_{AlN} \times x + D_{GaN} \times (1 - x) \quad (1)$$

Bandgap energies of strain-free AlGaN alloys were calculated using Vegard's law from the $E_g$ values of AlN and GaN listed in Table 3 of the main text using a bowing parameter, $b = 1$[1] as.

$$E_{g\,AlGaN} = E_{g\,AlN} \times x + E_{g\,GaN} \times (1 - x) + b \times x(1 - x) \quad (2)$$

For the more general case, AlGaN grown on $c$-plane GaN is subjected to a biaxial tensile strain due to the mismatch in lattice parameter $c$. The component of this biaxial strain is given by

$$\varepsilon_{xx} = \varepsilon_{yy} = (a_{GaN} - a_{AlGaN})/a_{AlGaN} \quad (3)$$

As a result of this biaxial in-plane tensile strain, a corresponding out-plane compressive strain is induced in the [0001] direction, which may be expressed in terms of the biaxial in-plane strain using the elastic constants as

$$\varepsilon_{zz} = -\frac{2C_{13}}{C_{33}}\varepsilon_{xx} \tag{4}$$

Now, using the biaxial in-plane and the out-of-plane strains, the bandgap energy of AlGaN pseudomorphically strained on *c*-plane GaN can be calculate as[2].

$$E_{g\,AlGaN} = E_{g\,AlGaN}(0) + (a_{cz} - D_1)\varepsilon_{zz} + (a_{ct} - D_2)\varepsilon_{\perp} - (D_3\varepsilon_{zz} + D_4\varepsilon_{\perp}) \tag{5}$$

where, $E_{g\,AlGaN}(0)$ is the bandgap energy of strain-free AlGaN obtained using Eq. (2), $\varepsilon_{\perp} = \varepsilon_{xx} + \varepsilon_{yy}$, and the deformation potentials ($a_{cz}$-$D_1$), ($a_{ct}$-$D_2$), $D_3$, $D_4$ are obtained using Eq. (1).

However, for the growth on nonpolar *m*-plane (1-100) surface, applicable to our AlGaN grown on GaN nanowire sidewalls, anisotropic in-plane tensile strains exist as $\varepsilon_{xx}$ along [11-20] and $\varepsilon_{zz}$ along [0001] due to lattice mismatch in *a* and *c* respectively. Fig. 5b in the main text depicts the orientation and notation *x*, *y*, *z* used in the present discussion, and is the same for previous discussion on *c*-plane oriented growth. The anisotropic in-plane strains in this case are determined from the lattice mismatch between GaN and AlGaN using Eq. (3) in the respective directions. The in-plane tensile strains induce a compressive strain on AlGaN, and from Fig. 5b, it may be understood that the out-of-plane compressive strain in this case is $\varepsilon_{yy}$ along the [1-100] direction. This out-of-plane compressive strain may be calculated using elastic constants as

$$\varepsilon_{yy} = -\frac{C_{11}}{C_{33}}\varepsilon_{xx} - \frac{C_{12}}{C_{33}}\varepsilon_{zz} \tag{6}$$

The bandgap energy of strained AlGaN on *m*-plane GaN may then be calculated using the deformation potentials as[2]

$$E_{g\,AlGaN}(1) = E_{g\,A/B}(0) + (D_2 + D_4)\varepsilon_{xx} + D_5\varepsilon_{xx}$$

$$E_{g\,AlGaN}(2) = E_{g\,A/B}(0) + (D_2 + D_4)\varepsilon_{xx} - D_5\varepsilon_{xx}$$

$$E_{g\,AlGaN}(3) = E_{g\,C}(0) + D_2\varepsilon_{xx} \tag{7}$$

Using Eq. (2), (5) and (7), the transition energies for strain-free AlGaN, AlGaN strained on *c*-plane GaN, and AlGaN strained on *m*-plane GaN have been calculated and plotted as Fig. 4b in the main text. Considering the case of AlGaN strained on *m*-plane GaN and the observed room temperature near band edge (NBE) emission peaks, we determined the Al composition

of AlGaN samples as 10.3, 15.0, 22.0, 30.5 and 40.2% respectively for Al-15, Al-20, Al-30, Al-40, and Al-50 and is listed in Table 2 of the main text. The compositions determined from cathodoluminescence (CL) measurements agree well with those determined from energy dispersive x-ray spectroscopy (EDS) as shown in Fig. 5a of the main text.

## 2. Partial dislocations in the samples Al-30 and Al-50

Fig. S1 shows HRTEM images of samples Al-30 and Al-50 and their corresponding Bragg-filtered images superimposed with strain maps. In-plane (Fig. S1b, e) and out-of-plane (Fig. S1c, f) strain maps overlaid on Bragg-filtered images clearly show an increase in formation of PDs with increasing Al content. The increase in PDs with Al content is expected in order to compensate the increased tensile strain experienced by *m*-plane AlGaN shell.

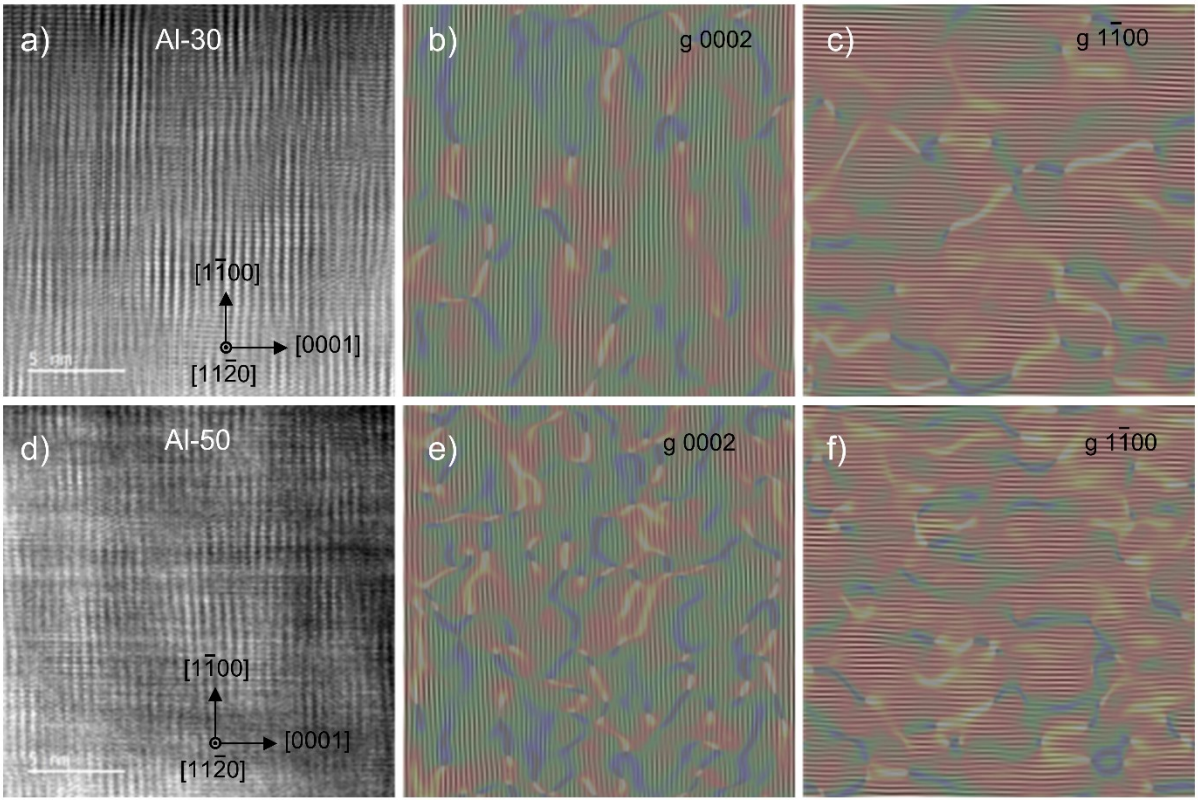


Fig. S1. (a, d) HRTEM images of AlGaN shell in samples Al-30 and Al-50. (b, e) In-plane strain maps overlaid on g(0002) Bragg filtered images for samples Al-30 and Al50, respectively. (c, f) Out-of-plane strain maps overlaid on g(1-100) Bragg filtered images for samples Al-30 and Al-50, respectively.

References

1. F. Yun, M. A. Reshchikov, L. He, T. King, H. Morkoc, S. W. Novak and L. Wei, *J. Appl. Phys.*, 2002, **92**, 4837-4839.
2. Q. Yan, P. Rinke, A. Janotti, M. Scheffler and C. G. Van de Walle, *Phys. Rev. B*, 2014, **90**, 125118.